Jpn. J. Appl. Phys. Vol. 41 (2002) pp. 7367–7372
Part 1, No. 12, December 2002

All-Optical Decision Gate with an Adjustable Decision Threshold

Jyh-Tsung HSIEH*, San-Liang LEE[1] and Jingshown WU

Graduate Institute of Communication Engineering and Department of Electrical Engineering, National Taiwan University, Taipei, Taiwan, R.O.C.
[1]*Department of Electronic Engineering, National Taiwan University of Science and Technologies, Taipei, Taiwan, R.O.C.*

(Received May 14, 2002; accepted for publication August 29, 2002)

We investigate the decision threshold adjustment in a proposed all-optical decision gate consisting of two gain-clamped semiconductor optical amplifiers (GCSOA's). The GCSOA discussed in this letter is constructed with a gain section and two passive distributed Bragg reflectors (DBR's) on each side. We derive a model for current-induced or temperature-dependent Bragg reflectance variation, with which the threshold current density and the oscillating power at DBR wavelength are described. This model allows a possible numerical prediction for decision threshold adjustment induced by current injection or temperature variation. [DOI: 10.1143/JJAP.41.7367]

KEYWORDS: all-optical decision gate, gain-clamped SOAs, decision threshold, thermal tuning, current tuning

1. Introduction

All-optical regeneration will be essential in future high-speed optical systems to suppress the accumulation of noise and jitter, which severely limit the network node cascadability. Several techniques for all-optical regeneration have been investigated, and some of the most promising results have been achieved with interferometric wavelength converters (IWCs).[1,2] In these devices, 2R regeneration is accomplished due to the nonlinear transfer function of the converter.[3] However, the amplitude imbalance decreases the extinction ratio of the interferometer. Very recently, improved regeneration was proposed utilizing an interferometric structure incorporating gain-clamped SOAs (GCSOAs) as phase shifters.[4–6]

The gain saturation induced non-linearity generates crosstalk which is a severe limitation for the use of SOAs in wavelength division multiplexer (WDM) based systems. In contrast, GCSOA has a gain that is constant with respect to input power variation, as long as the amplified signal power is less than the oscillating power, leading to a flat gain versus output power response. The coupling with the lasing mode also results in a readjustment in carrier density by relaxation oscillations. Moreover, playing with the feedback level of the reflectors which determines the gain of the GCSOA, and considering a given output power, it is possible to maintain the gain at a moderate value so as to increase again the dynamic input power range. The improved dynamic response in GC SOA's facilitates the achievement of an all-optical decision gate.

Considering the distinct input signal level, a decision gate with an adjustable decision threshold is thus required. Öberg *et al.*[7] have reported a tunable DBR laser that is tuned via heating. The principle of using local heating of passive sections in DBR lasers is based on refractive index change caused by temperature variation. Even though this tuning method is not as fast as tuning by carrier injection, it does have certain important advantages—it neither degrade the output power nor the linewidth, as much as tuning employing carrier injection.

As an alternative method, the adjustment of the decision threshold can be done by an electronic control of the wavelength-selective filtering element, namely the Bragg reflector. The electronic variation of the refractive index of the grating region may thus be employed to accomplish the tuning of the cavity gain characteristic by tuning the wavelength-dependent mirror loss $\alpha_m(\lambda)$.

We have reported a GCSOA structure with two integrated Bragg gratings as wavelength selective reflectors.[8] The coupling coefficient of the grating is chosen so that it provides a high single pass gain at the oscillation threshold. By incorporating the GCSOA's into a Mach–Zehnder interferometer (MZI) structure an all-optical decision gate (AODG) is thus constructed. The device structure to be simulated is schematically shown on the insert in Fig. 2(b). The GCSOA's act as traveling-wave amplifiers in this case. Assuming homogeneous broadening of semiconductor gain lineshape, its overall gain is expected to be clamped once the threshold oscillation is reached. The GCSOA is a 3-section device that consists of a central gain section and two passive sections. Each passive section includes a distributed grating reflector so as to form a distributed Bragg reflector (DBR) cavity. The length is $2 \times L_g = 200\,\mu$m for the passive sections and $L_{ac} = 400\,\mu$m for the active section. The coupling coefficient (κ) of the grating will affect the extent of gain saturation.

We chose a $\kappa \times L_g$ value (L_g is the grating length) to produce about 6.5 dB fiber-to-fiber gain at 1550 nm. The gain curve with respect to the signal output power is reported in Fig. 1. The Bragg wavelength was fixed to 1510 nm so as

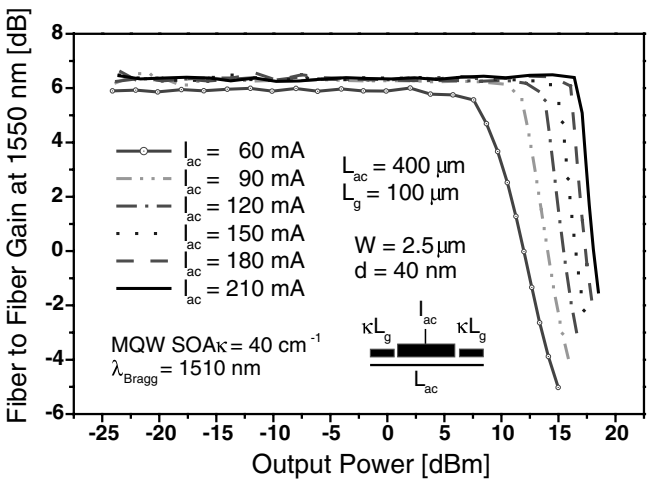

Fig. 1. Gain versus output power of DBR GC SOA.

*E-mail address: jyh_tsung@pchome.com.tw

to advance the filtering of the oscillating wavelength, taking into account that WDM applications imposes at 1530–1560 nm operating window. At a wavelength different from the Bragg wavelength, the gain is independent of the signal intensity as long as the lasing oscillation is not switched off through carrier depletion effect. A flat gain is observed for up to 15 dBm output power at 120 mA of injection current.

In this paper two methods for wavelength tuning of semiconductor lasers are examined to demonstrate the possibility of obtaining an adjustable decision threshold in an all-optical decision gate. For thermal tuning, we derive a simple model using a non-uniform temperature distribution along the DBR section of the device to describe the Bragg reflectance and spectral shift. On the other hand, the free-carrier plasma effect is used to control the refractive index of a Bragg reflector in the case of current tuning. Based on these two models, we successively predict the decision threshold in an all-optical decision gate.

2. Simulation Results

The simulations have been performed using a commercial software package,[9] which uses powerful and flexible laser models based on the Transmission-Line Laser Model (TLLM).[10] The DBR-GCSOA under investigation was assumed to be multiple quantum well (MQW) devices with a 40 nm $Ga_xIn_{1-x}As_yP_{1-y}$ MQW's embedded in InP waveguide core with a 210 nm separate confinement heterostructure (SCH) region. We summarize the parameters and their numerical values used in the simulation in Table I. The symbols in the parentheses denote the parameters in the following theoretical analysis.

The structure of the MZI-based reshaping device is constructed with symmetric couplers and identical GCSOA's in both arms. The GCSOA's are assumed to be completely identical and to have a different bias current. They, therefore, give an identical and constant amplification and phase shift below the saturation power, but they exhibit a different saturation power. In the linear regime, both arms of the MZI give the same signal gain and a constant phase delay. If we compensate the phase delay, a completely destructive interference below the input saturation powers of both GCSOA's is obtained at the output of the MZI. Beyond the saturation power of both GCSOA's, the phase difference between both arms is also constant, and the output powers from both GCSOA's are saturated, such that a constant output power is also obtained at the output of the MZI and hence a digital-like decision characteristic is achieved with the MZI regenerator. Calculated characteristics of two GCSOA's with different bias are shown in Fig. 2(a). As can be seen from the figure, the transfer function for this regeneration scheme is close to that of a decision gate. The turning points of regeneration characteristic depend on the bias current I_1 and I_2 of the two GCSOAs. Changing one or both of the bias currents would allow the adjustment of the decision threshold and/or the slope of the decision characteristic.

Table I. GCSOA parameters used in the numerical simulations.

Parameter	Value	Unit
Active region width (w)	2.5×10^{-6}	m
Active layer thickness (d)	0.04×10^{-6}	m
Internal loss (α_{ac})	3000	m^{-1}
MQW confinement factor (ξ_{ac})	0.07	—
SCH confinement factor (ξ_{SCH})	0.56	—
Group effective index (n)	3.7	—
Bimolecular recombination coefficient (B)	1.0×10^{-16}	m^3/s
Auger recombination coefficient	1.3×10^{-41}	m^6/s
Linear material gain coefficient	3×10^{-20}	m^2
Transparency carrier density	$1.5 \times 10^{+24}$	m^{-3}
Carrier capture time constant	70×10^{-12}	s
Carrier escape time constant	140×10^{-12}	s
MQW differential refractive index	-1.11×10^{-26}	m^3

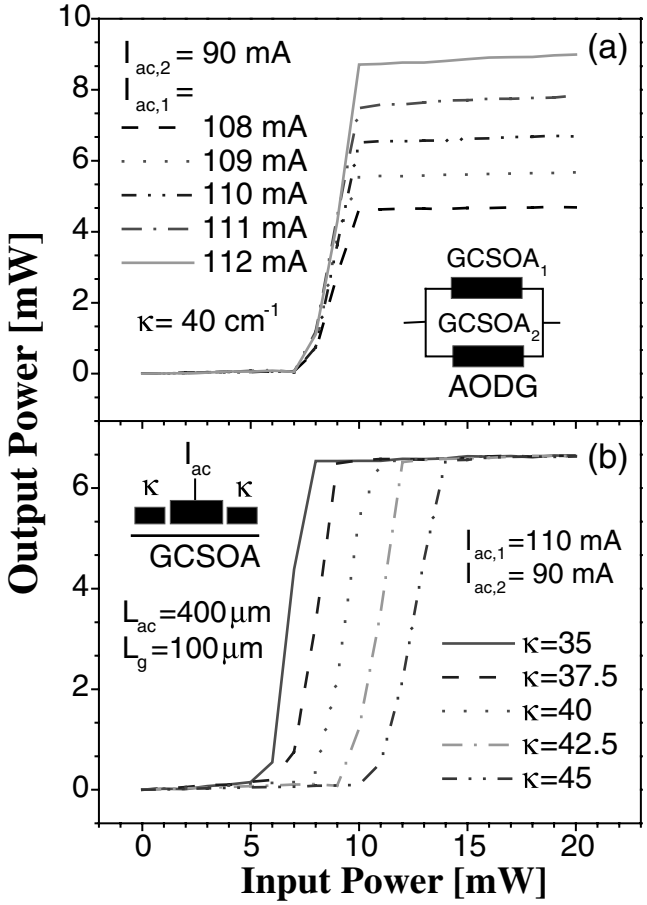

Fig. 2. (a) Output power versus input power of a decision gate for various I_1. (b) Output power versus input power of a decision gate for various κ values.

The 2R regeneration function of this decision gate is demonstrated in Fig. 3. In the time-domain simulation with a PRBS sequence of intentionally distorted pulses as input, the decision gate works very well at bit rates below 2.5 Gbit/s. Above 2.5 Gbit/s, however, degraded signal regeneration will result. The optical power, in fact, stored in the lasing wavelength and converted into amplified signal following intensity modulation, with a time response limited by the relaxation oscillation frequency. In order to apply the regenerator to higher-speed signals, one must optimize the GCSOA structure to raise the relaxation oscillation frequency and reduce the linewidth enhancement factor.[5]

At the Bragg wavelength, the magnitude of the field and power reflections depends only on $\kappa \times L_g$: $|r_g| \sim \tanh(\kappa L_g)$

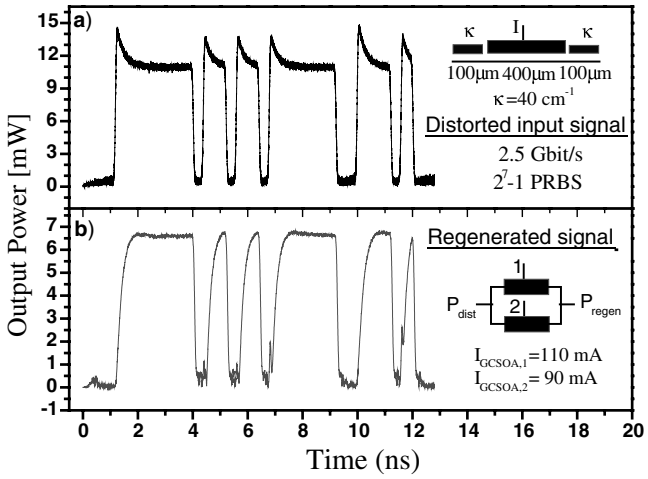

Fig. 3. Time evolution of the distorted and regenerated signals for a 2.5 Gbit/s $2^7 - 1$ PRBS bit sequence.

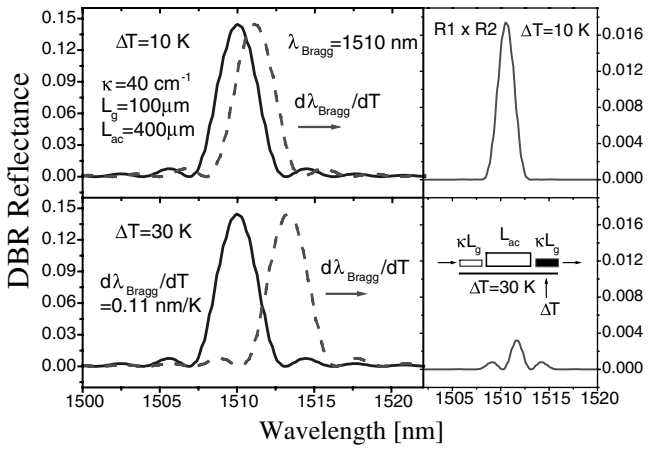

Fig. 4. Schematic representation of the temperature dependencies of both Bragg peaks in a GCSOA.

and $R_g = |r_g|^2 \sim \tanh^2(\kappa L_g)$. To expand the decision threshold adjustment, we thus tried the simulations in which the $\kappa \times L_g$ value in a GCSOA has been varied. Figure 2(b) shows these results and it is clearly seen that about 5 mW threshold downshift can be attained through the reduction of κ from 45 to 35 cm^{-1}. Quite reasonably, the decreased decision threshold is ascribed to the reduced reflectivity in the DBR grating with a smaller κ. With this observation, we are encouraged to design an all-optical decision gate with an adjustable decision threshold.

3. Theoretical Analysis

Due to the varying input signal levels, tunable decision gates are required in practical optical communication system. To meet the requirements, thermal or current tuning of decision threshold in an all-optical decision gate is explored through the individual model analysis.

3.1 Thermal tuning

It's well known that the Bragg reflectance of a DBR grating will change with temperature since its refractive index varies with temperature. A worse overlap of both Bragg reflection peaks, based on temperature-dependent spectral shift, will require a higher threshold current in a DBR laser. Taking advantage of these characteristics, tunable decision gates can hence be attained by locally heating the DBR grating section to acquire different spectral overlap. Selectively heating the Bragg section moves the center wavelength of the wavelength-selective mirror. Tuning only one of both Bragg sections through resistive heating will separate both DBR mirrors, leading to a reduced reflectivity. To see this explicitly, we will calculate the temperature tuning rate of Bragg peak using simple models for the wavelength-dependent reflectivity. The Bragg reflectance curve, $R(\lambda, T)$, can be expressed as

$$R(\lambda, T) = \left| \frac{-j\kappa \cdot \sinh(\gamma L_g)}{\gamma \cdot \cosh(\gamma L_g) + (\alpha + j\Delta\beta) \cdot \sinh(\gamma L_g)} \right| = |r| e^{j\phi}. \tag{1}$$

with L_g being the grating length, $\gamma = \sqrt{\kappa^2 + (\alpha + j\Delta\beta)^2}$ and

$$\Delta\beta = \beta - \beta_0 = 2\pi n_{\mathrm{eff}} \left(\frac{1}{\lambda} - \frac{1}{\lambda_{\mathrm{Bragg}} + \dfrac{d\lambda_{\mathrm{Bragg}}}{dT} \cdot \Delta T} \right). \tag{2}$$

In this expression, typical numerical values are $n_{\mathrm{eff}} = 3.7$, $\lambda_{\mathrm{Bragg}} = 1510\,\mathrm{nm}$, $d\lambda_{\mathrm{Bragg}}/dT = 0.11\,\mathrm{nm/K}$,[11] $L_g = 100\,\mu\mathrm{m}$, and $\kappa = 40\,\mathrm{cm}^{-1}$.

The resultant temperature tuning characteristics are shown in Fig. 4 for a GCSOA. The effective length of the Bragg section varies with temperature, and, more importantly, the Bragg peak is also changing. When the entire GCSOA is heated, the length of the cavity and the Bragg peak tune at approximately the same rate, so that no mode hops occur; but if one heats just the Bragg section, then mode hops will occur. However the laser will emit light in the longitudinal mode with the wavelength closest to the Bragg peak wavelength, and the laser wavelength will always be close, though not necessarily equal, to the Bragg wavelength. Resorting to these behaviors, the lasing power will decrease with the temperature increases. The saturation power is thus reduced and a decrease on decision threshold of a decision gate is attained.

Next, let us consider the dependence of the threshold current density on device temperature. Using the complex reflectivities of DBR's by (1), the threshold condition of a DBR laser is written as

$$\begin{aligned} (\sqrt{C_{\mathrm{out}}})^4 |r_1||r_2| \exp[j(\phi_1 + \phi_2 - 2\bar{\beta} L_{\mathrm{ac}})] \\ \times \exp[(\xi_{\mathrm{ac}} g_{\mathrm{th}} - \bar{\alpha}) L_{\mathrm{ac}}] = 1. \end{aligned} \tag{3}$$

where C_{out} is the coupling coefficient between the active region and the DBR region, L_{ac} is the length of the active region, $\bar{\alpha}$ is the loss in the active region, $\bar{\beta} = 2\pi\overline{n_{\mathrm{eff}}}$, and the suffixes 1 and 2 are used to distinguish two DBR's. From (3), threshold gain is given as

$$\xi_{\mathrm{ac}} g_{\mathrm{th}} = \bar{\alpha} + \frac{1}{L_{\mathrm{ac}}} \left(\frac{1}{2} \ln \frac{1}{R_1 R_2} + 2 \ln \frac{1}{C_{\mathrm{out}}} \right) \tag{4}$$

where $R_{1,2} = |r_{1,2}|^2$. Accordingly, the threshold current density is derived from the relation of $J_{\mathrm{th}} \propto g_{\mathrm{th}}^2$ as

$$J_{\mathrm{th}} = \frac{ed}{n_o \tau_{\mathrm{T0}}} \left(\frac{1}{A_o \xi_{\mathrm{ac}}} \right)^2 \cdot g_{\mathrm{th}}^2$$

$$= \frac{d}{1.56\xi_{ac}^2}\left\{\bar{\alpha} + \frac{1}{L_{ac}}\left(\frac{1}{2}\ln\frac{1}{R_1R_2} + 2\ln\frac{1}{C_{out}}\right)\right\}^2 (\mathrm{kA/cm^2}) \quad (5)$$

where $\bar{\alpha} = \alpha_{ac}\xi_{ac} + \alpha_{SCH}\xi_{SCH}$.[12] d is the thickness of the active layer, ξ_{ac} and ξ_{SCH} are the confinement factors in the active layer and the output guide, respectively, and α_{ac} and α_{SCH} are the free carrier absorption loss in the active layer and the output guide layers, respectively. The notations in the first part of (5) are subject to those in ref. 12. In (5), the term $\ln(1/R_1R_2)$ gives wavelength selectivity due to thermal tuning of DBR reflectance. The temperature dependence of threshold current density as a function of the coupling coefficient is shown in Fig. 5. Obviously, thermal induced separation for two grating mirrors causes threshold current to increase as a result of reduced mirror reflectivity.

Inspection of Fig. 5 clearly identifies the effect of coupling coefficient on threshold current density. Due to the symmetric grating structures, same purposes can be attained by either elevating or descending the grating temperature. Results also indicate that the threshold condition of a DBR laser with a larger coupling coefficient is less affected by varying the grating temperature. Note that the change in the lasing wavelength takes a form approximate to

$$\lambda_{Bragg} + \frac{1}{2}\frac{d\lambda_{Bragg}}{dT}\cdot\Delta T.$$

In tuning the Bragg reflector, mode hopping might occur due to the change in the round-trip phase inside the GCSOA. Here we neglect the mode hopping problem in order to simplify the discussion. Furthermore, in most case, the GCSOA will self-adjust its phase status against the change in material parameters to meet the requirements for the least threshold condition.

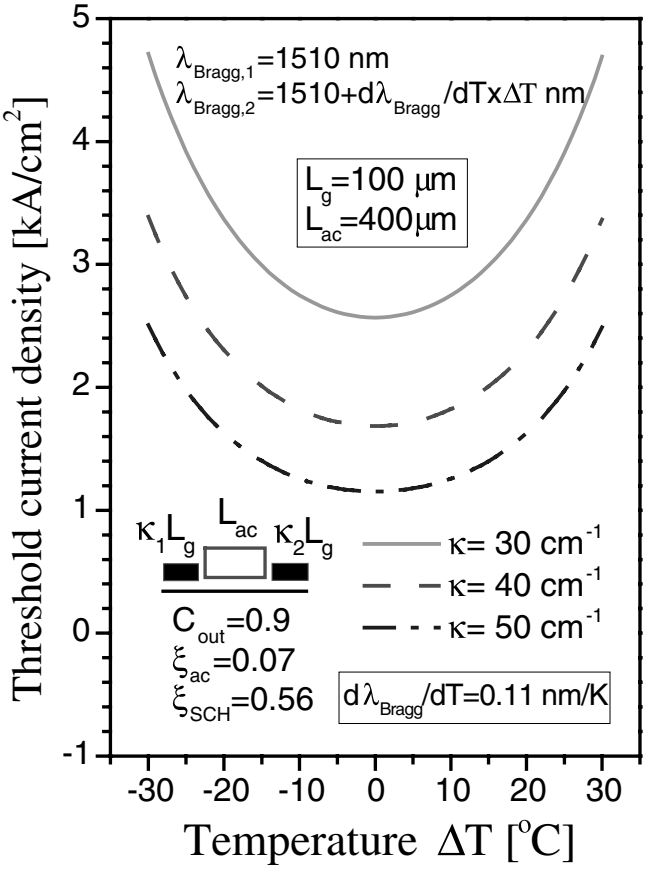

Fig. 5. Temperature-dependent threshold current density J_{th} as calculated by (5) as a function of coupling coefficient.

Subsequently, the internal lasing power at DBR wavelength is examined to determine decision threshold and its dependence on grating temperature. If the differential quantum efficiency inside the cavity is given as[12]

$$\eta_{d,int} = \eta_i \frac{\frac{1}{2}\ln\frac{1}{R_1R_2}}{(\bar{\alpha} - \alpha_{in}\xi_{ac})L_{ac} + \frac{1}{2}\ln\frac{1}{R_1R_2} + 2\ln\frac{1}{C_{out}}}, \quad (6)$$

then the internal lasing power at the Bragg wavelength can be expressed as,

$$P_{las,int} = \frac{hv}{q}\eta_{d,int}(J - J_{th})WL. \quad (7)$$

where η_i is the internal quantum efficiency and W and L are width and length of active layer, separately. Above threshold, η_i is normally believed to be unity.

In a DBR laser, the threshold current density is a function of DBR reflectance that is strongly dependent on the coupling coefficient of the DBR gratings. With the coupling strength increases, the threshold current density reduces because of an enhanced Bragg reflectance. This growth of the output power of the DBR laser results in the improvement of saturation power. The internal lasing power is mainly a function of injection current and grating temperature, as shown in Fig. 6. Degraded internal quantum efficiency mostly elucidates the suppressed internal lasing power at large coupling strengths. The calculated results resemble the observation in our previous simulation [Fig. 2(b)], if we assume that the decision threshold will occur when the amplified signal power in a GCSOA is equal to the internal lasing power at DBR wavelength.

Further to above discussion, we can use (7) to build a relationship between the internal lasing power and temperature change for thermally tuning the decision threshold. As can be seen in Fig. 7, the lasing power exhibits a nonlinear dependence on temperature. The tuning range attains to 35°C, which corresponds to about 3.8 nm of peak separation for both DBR gratings. Accordingly, threshold condition will boost as soon as the amplified signal power surpasses the internal lasing power. For this reason, an excess cavity gain must be excluded to account for the signal amplification. While considering two mirror losses and neglecting the gain compression induced by thermal, we calculate the cavity gain as 8.5 dB in the case of $\kappa = 40\,\mathrm{cm^{-1}}$. Then the decision threshold can be determined as shown in Fig. 7. The discrepancy in the threshold power is mainly caused by an ignorance of dynamic carrier interchange between laser mode and amplifier mode. Incorrect estimation of material and structure loss which are hardly to be determined in our case could lead to another possibility for threshold deviation.

To see the thermal effect more clearly, the correspondence between the spectrum shift and temperature rise is also plotted in Fig. 7. For the device with $\kappa = 40\,\mathrm{cm^{-1}}$, 1 dB

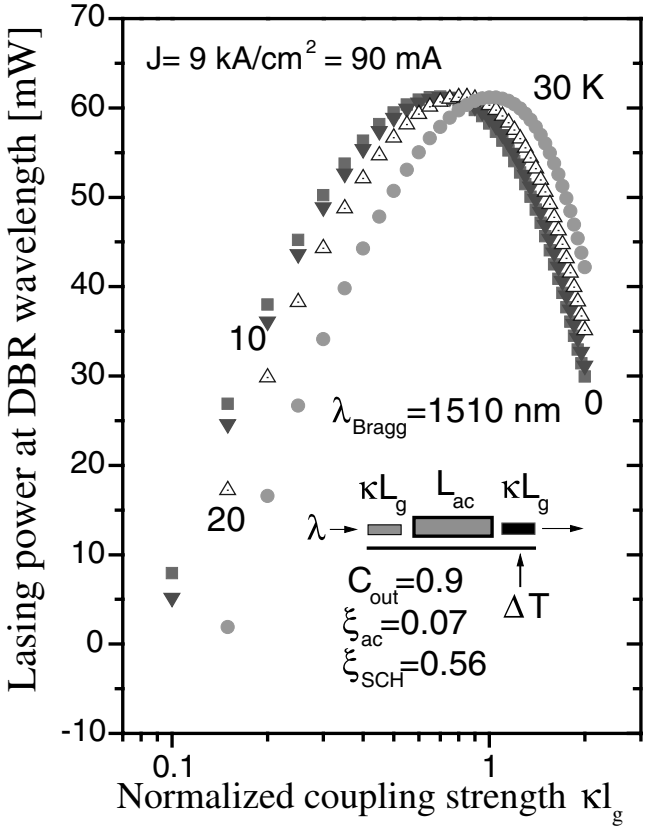

Fig. 6. Internal lasing power as a function of normalized coupling strength at different grating temperature.

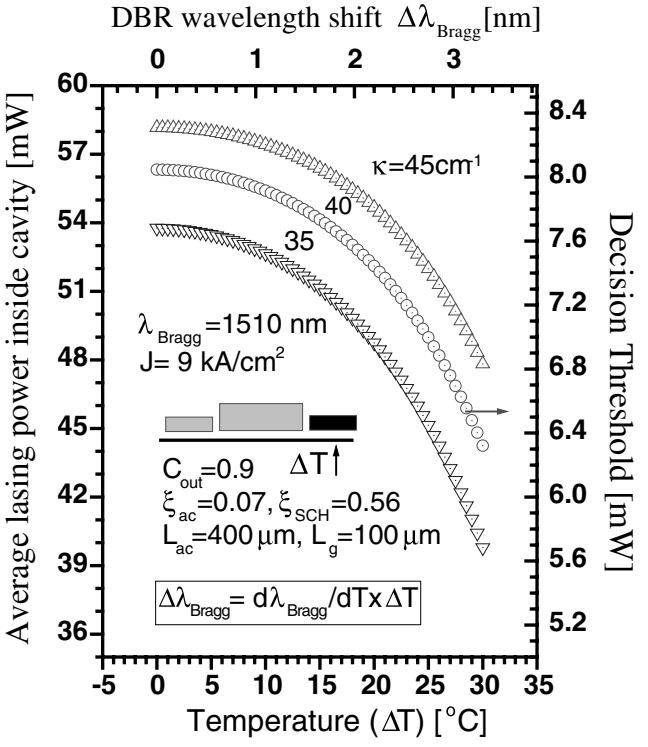

Fig. 7. Thermal tuning induced change in the internal lasing power of a GCSOA.

reduction in decision threshold accompanies a peak wavelength shift of about 3.25 nm in heated grating section. The wavelength shift properly manifests the thermally

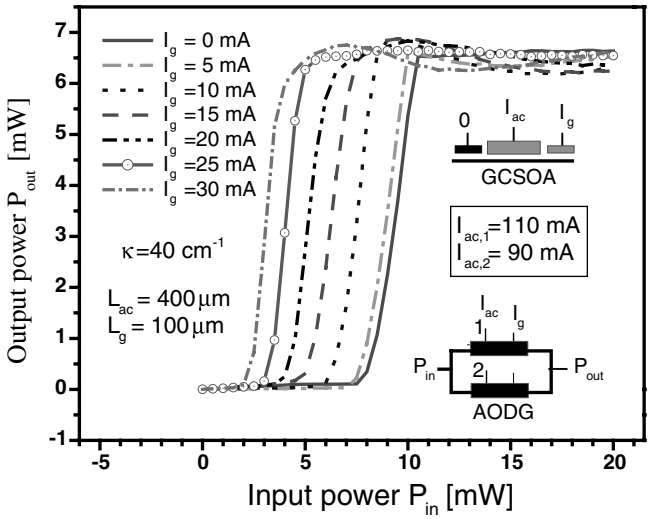

Fig. 8. Decision threshold adjustment of a decision gate by injecting various current into one of both DBR grating sections.

tunable characteristics for a DBR laser diode. On the other hand, while taking into account the coupling effect as in Fig. 5, a better temperature tuning is obtained by using a GCSOA with a smaller κ. This guideline also holds for the noise suppression in general GCSOA's.[13)]

3.2 Current tuning

The same effect of misaligning the two grating mirrors of a GCSOA can be obtained by tuning one of the grating sections with current injection. This approach can have the merit of fast tuning speed. The transfer characteristic of an AODG is displayed in Fig. 8 for a variety of injection current. The GCSOA enables the electronic control of the spectral shape of the cavity gain by the tuning of the Bragg wavelength over current I_g. By applying a control current to the Bragg section, its index, n_{DBR}, changes, and the center wavelength of the grating, λ_B, moves according to $\Delta\lambda_B/\lambda_B = \Delta n_{DBR}/n_{DBR}$. The resultant variation in DBR reflectance will adjust the threshold current density, which in turn determines the decision threshold of an AODG. In addition, we notice that refractive index change in grating section leads to reflectance spectrum shift in both cases of thermal tuning and current injection. With this finding, we can estimate these two tuning methods by correlating the decision threshold with the common variable $\Delta\lambda_B$-DBR wavelength shift.

The wavelength shift of the grating vs. the tuning current can be derived as eq. (8) with only radiative recombination is anticipated in carrier dynamics.[14)]

$$\Delta\lambda_B = \lambda_B \frac{\Gamma_{xy} \cdot 10^{-26}}{n_g} \left[\frac{\eta_i I_g}{qVB}\right]^{1/2} \cong 1.2\sqrt{I_g} \quad \text{(nm)} \qquad (8)$$

where Γ_{xy} is the confinement factor for the passive 0.46 μm guide, n_g is the average refractive index in grating section, V is the volume of grating section, and B is the bimolecular recombination coefficient. Fig. 9 gives the plot of decision threshold vs. grating tuning current as well as the corresponding wavelength shift. The decision threshold is linearly dependent on the grating current with a negative slope. After transformation using eq. (8), a relevant curve

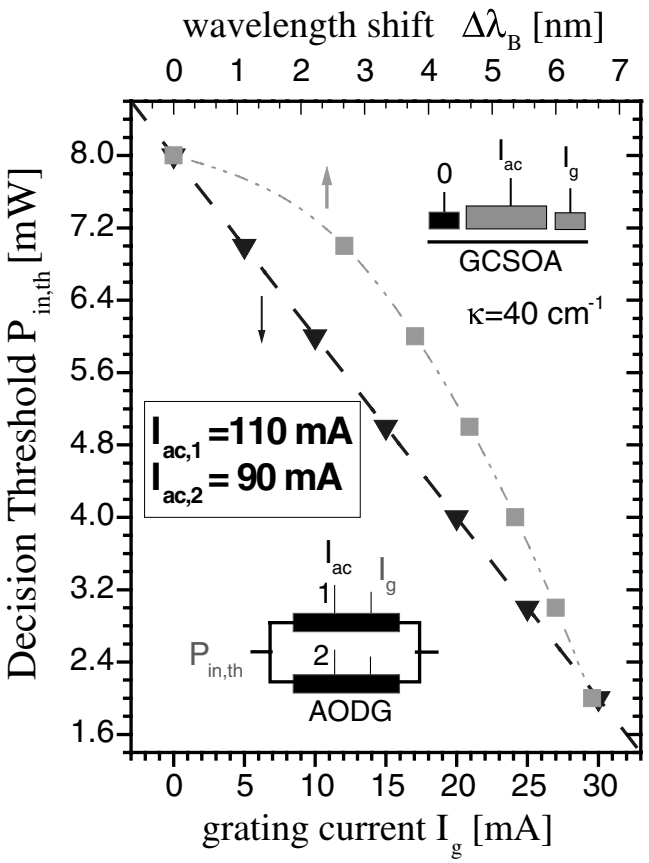

Fig. 9. Decision threshold of decision gate vs. Bragg tuning current of GCSOA. The wavelength shift of grating is calculated by eq. (8) with the following parameter values: $\Gamma_{xy} = 0.49$, $n_g = 4.0$, $\eta_I = 0.8$, $V = 100 \times 2.5 \times 0.46\,\mu\text{m}^3$, $B = 1 \times 10^{-16}\,\text{m}^3/\text{s}$.

similar to that in Fig. 7 is obtained. Approximately, an adjustment of 1 dB in decision threshold acquires about 3.2 nm DBR wavelength shift. The outcome is in consistent with our calculated results using a simplified thermal model. Therefore, in predicting the decision threshold adjustment by thermal or current tuning, our numerical method is proven to be effective.

4. Conclusions

We construct an all-optical decision gate and examine if an adjustable decision threshold is available via resistive local heating and/or current injection of passive section in GCSOA. A model dealing with the temperature-dependent gain spectrum and DBR reflectance is derived to predict the simulated decision threshold. The decision threshold of a Mach–Zehnder decision gate is in response to the saturation of the output power of a GCSOA, which is caused by the annihilation of laser operation at Bragg wavelength. Based on this assumption, we have explored the dependences of threshold current density and internal differential quantum efficiency on temperature variation. The lasing power at Bragg wavelength and thus the threshold condition can be determined by varying the device temperature. In addition, tuning by carrier injection into just one DBR grating section is also studied as an alternative depending on its fast response and ease of operation. Quite consistent results between these two tuning methods verify the effectiveness of our simplified thermal model. Consequently, we can design an all-optical decision gate with an adjustable decision threshold either by current injection or locally resistive heating the Bragg grating region.

Acknowledgment

Part of this work is supported by the National Science Council and the Ministry of Education, Taiwan, R.O.C. under Grants NSC90-2215-E-002-012 and 89E-FA06-2-4-7.

1) D. Chiaroni, B. Lavigne, A. Jourdan, L. Hamon, C. Janz and M. Renaud: Proc. ECOC'97, Edinburgh, UK, 1997, Vol. 5, p. 41.
2) B. Lavigne, D. Chinroni, L. Hamon, C. Janz and A. Jourdan: Tech. Dig. OFC'98, San Jose, USA, 1998, Paper Th07.
3) D. Wolfson, B. Mikkelsen, S. L. Danielsen, H. N. Poulsen, P. B. Hansen and K. E. Stubkjaer: Tech. Dig. OFC'98, San Jose, USA, 1998, Paper WB3.
4) G. Morthier, J. Sun, T. Gyselings and R. Beats: Tech. Dig. OFC'98, San Jose, USA, 1998, Paper WM19.
5) G. Morthier, J. Sun, T. Gyselings and R. Beats: IEEE Photonics Technol. Lett. **10** (1998) 1162.
6) G. Morthier, M. Zhao, B. Vanderhaegen and R. Beats: IEEE Photonics Technol. Lett. **12** (2000) 1516.
7) M. Öberg, S. Nilsson, T. Kligna and P. Ojala: IEEE Photonics Technol. Lett. **3** (1991) 299.
8) J. T. Hsieh, S. L. Lee and J. Wu: 2nd Int. Laser, Lightwave and Microwave Conf. (ILLMC2001), Shanghai, China, 2001.
9) VPItransmissionMaker™ Active Photonics simulation suite.
10) A. Lowery, O. Lenzmann, I. Koltchanov, R. Moosburger, R. Freund, A. Richter, S. Georgi, D. Breuer and H. Hamster: IEEE J. Sel. Top. Quantum Electron. **6** (2000) 282.
11) J. J. Dudley, D. L. Crawford and J. E. Bowers: IEEE Photonics Technol. Lett. **4** (1992) 311.
12) M. Asada, A. R. Adams, K. E. Stubkjaer, Y. Suematsu, Y. Itaya and S. Arai: IEEE. J. Quantum Electron. **17** (1981) 611.
13) J. Sun, G. Morthier and R. Baets: IEEE J. Sel. Top. Quantum Electron. **3** (1997) 1162.
14) L. A. Coldren and S. W. Corzine: *Diode Lasers and Photonic Integrated Circuits* (John Wiley & Sons, 1995) Chap. 8, p. 349.